

## Emergence of Highly Degenerate Excited States in the Frustrated Magnet $\text{MgCr}_2\text{O}_4$

K. Tomiyasu,<sup>1,\*</sup> T. Yokobori,<sup>2</sup> Y. Kousaka,<sup>2</sup> R. I. Bewley,<sup>3</sup> T. Guidi,<sup>3</sup> T. Watanabe,<sup>4</sup> J. Akimitsu,<sup>2</sup> and K. Yamada<sup>5</sup>

<sup>1</sup>*Department of Physics, Tohoku University, Aoba, Sendai 980-8578, Japan*

<sup>2</sup>*Department of Physics and Mathematics, Aoyama-Gakuin University, Sagamihara 229-8558, Japan*

<sup>3</sup>*ISIS Facility, Rutherford Appleton Laboratory, Chilton, Didcot OX11 0QX, United Kingdom*

<sup>4</sup>*Department of Physics, College of Science and Technology (CST), Nihon University, Chiyoda, Tokyo 101-8308, Japan*

<sup>5</sup>*Institute of Materials Structure Science, High Energy Accelerator Research Organization, Oho, Tsukuba 305-0801, Japan*

(Received 9 September 2012; published 15 February 2013)

High degeneracy in ground states leads to the generation of exotic zero-energy modes, a representative example of which is the formation of molecular spin-liquid-like fluctuations in a frustrated magnet. Here we present single-crystal inelastic neutron scattering results for the frustrated magnet  $\text{MgCr}_2\text{O}_4$ , which show that a common set of finite-energy molecular spin excitation modes is sustained in both the liquid-like phase above magnetic ordering temperature  $T_N$  and an ordered phase with an extremely complex magnetic structure below  $T_N$ . Based on this finding, we propose the concept of high degeneracy in excited states, which promotes local resonant elementary excitations. This concept is expected to have ramifications on our understanding of excitations in many complex systems, including not only spin but also atomic liquids, complex order systems, and amorphous systems.

DOI: [10.1103/PhysRevLett.110.077205](https://doi.org/10.1103/PhysRevLett.110.077205)

PACS numbers: 75.25.Dk, 63.50.-x, 75.40.Gb, 78.70.Nx

The concept of elementary excitations, or quasiparticles, constitutes the basis of modern condensed matter physics [1]. Intricate interactions among a large number of particles, like in liquids, can be successfully treated as a collection of independent quasiparticles; examples include magnons, phonons, and rotons arising from helium superfluids [2]. In addition, magnetic pseudomonopoles, which have been long sought after in high-energy physics, were recently observed as elementary excitations in a spin-liquid-like phase in a highly frustrated magnet called a spin ice [3]. Thus, studying elementary excitations in complex systems like liquids could have broad implications across many fields of physics.

Highly frustrated magnets are promising sources for exotic spin-liquid-like states. This is because in frustrated magnets, not all classical-spin pairs can be arranged antiferromagnetically on a triangular or tetrahedral lattice, which gives rise to an inherent macroscopic degeneracy in ground states [4,5]. Therefore, in a temperature region that is sufficiently lower than a magnetic interaction scale, frustration suppresses magnetic ordering and promotes spin-liquid-like fluctuations (zero-energy modes), which are accompanied by short-range spatial correlations that lower system entropy, as required by the third law of thermodynamics ( $L$  phase). A representative example of this phenomenon is the formation of molecular spin-liquid-like fluctuations, where a spin molecule refers to a spin cluster that is spatially confined within a geometrical region, such as an atomic molecule. For example, in the spinel antiferromagnet  $\text{MgCr}_2\text{O}_4$  ( $T_N = 13$  K,  $\theta_{CW} = -370$  K [6]), the magnetic ions  $\text{Cr}^{3+}$  [ $(t_{2g})^3$ , spin  $S = 3/2$ ] form a corner-sharing tetrahedral lattice called a pyrochlore lattice, as shown in Fig. 1(a), and the  $L$  phase

(above  $T_N$ ) exhibits antiferromagnetic spin hexamers [7], as shown as the first mode in Fig. 1(b). The hexamers correspond to a characteristic neutron scattering intensity pattern that is widely spread along the Brillouin zone boundary of the lattice structure [7], as shown in the bottom-left corner panel in Fig. 1(b), which is reproduced by classical-spin Monte Carlo simulations [8].

Notably, there is little available information on *finite-energy* elementary excitations in this molecular  $L$  phase; in fact, there is no experimental report in existence. This is probably because zero-energy modes are one of the most important phenomena directly resulting from frustration. Indeed, many studies on frustrated magnets in the  $L$  phase were focused solely on the zero-energy modes [7,9–12].

By contrast, in the magnetically ordered phase ( $O$  phase) in several spinel antiferromagnets, where frustration was assumed to be relieved by a lattice distortion, molecular spin and spin-orbit resonances were recently discovered to exist as nondispersive gapped elementary excitation modes [7,11,13]. An  $O$  phase in  $\text{MgCr}_2\text{O}_4$  exhibits a complex tetragonal spin-lattice order that is essentially equivalent to that in  $\text{ZnCr}_2\text{O}_4$  [14,15], and the hexamer mode and a heptamer mode [the first and second modes in Fig. 1(b)] are observed at 4.5 and 9.0 meV, respectively [7]. Interestingly, the heptamer-type zero-energy mode is also observed in an  $L$  phase in another frustrated pyrochlore magnet  $\text{Tb}_2\text{Ti}_2\text{O}_7$  [12], and a ground state composed of the same structural units is observed in a frustrated spinel magnet  $\text{AlV}_2\text{O}_4$  with charge degree of freedom [16].

In this Letter, we explored finite-energy excitations in the  $L$  phase and clarified their relation with those in the  $O$  phase through a comprehensive study of spin excitations

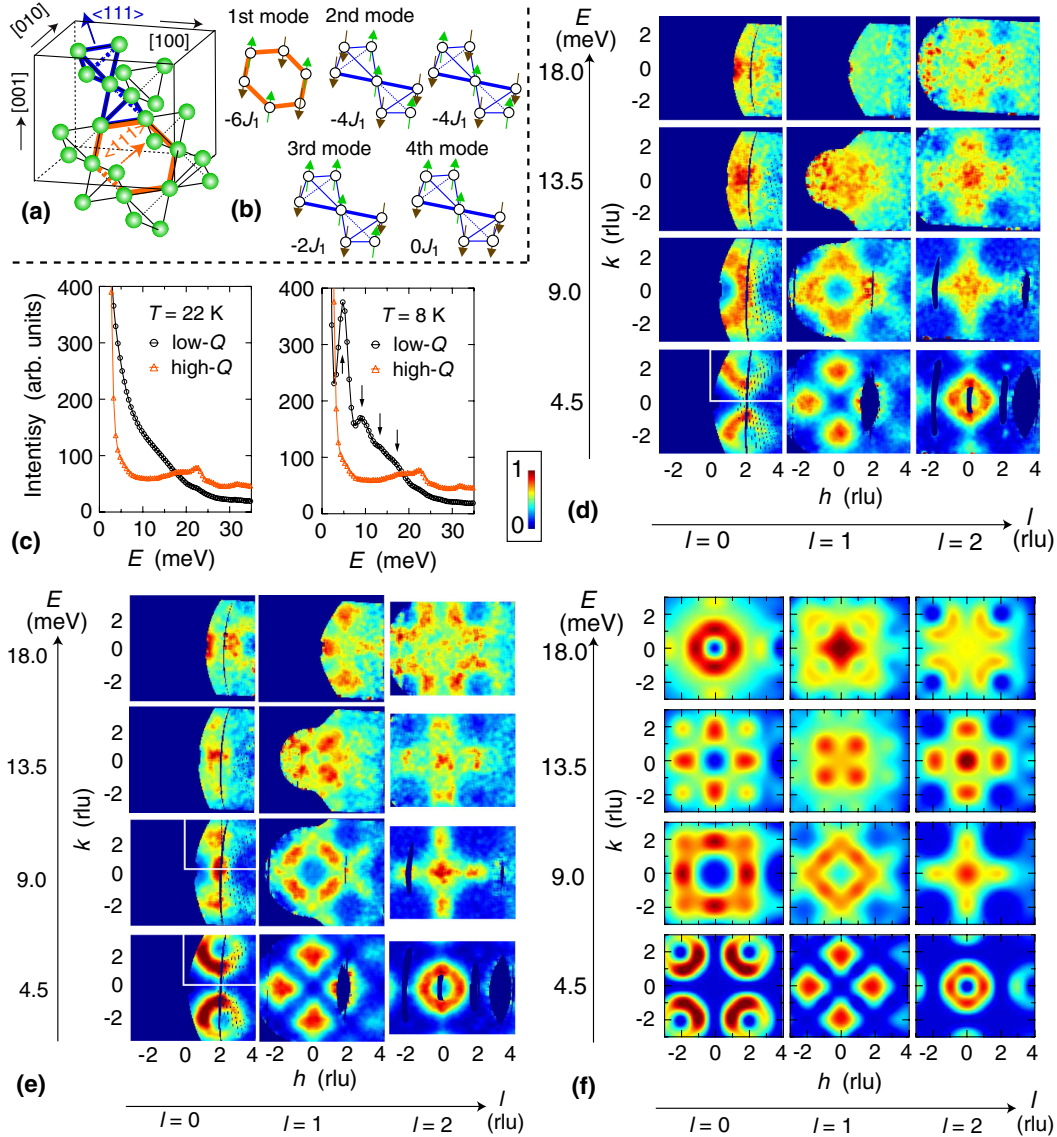


FIG. 1 (color online). (a) Pyrochlore lattice. The bold lines mark examples of positions of the hexamer and heptamers shown in (b) among equivalent positions. (b) Snapshots of spin molecular models. The arrows indicate spins, which dynamically fluctuate in arbitrary directions in keeping with the relative correlations. The total exchange interaction energies in the molecules are also shown, where  $J_1$  is the magnitude of the nearest-neighbor exchange interaction energy. (c)  $E$  dependence of  $Q$ -integrated intensity measured in an  $L$  phase (left panel) and  $O$  phase (right panel). The integration ranges are  $0 < h < 2$ ,  $0 < k < 2$ , and  $0 < l < 2$  reciprocal lattice units (rlu) in the low- $Q$  data and  $0 < h < 2$ ,  $5 < k < 7$ , and  $0 < l < 2$  rlu in the high- $Q$  data. The arrows indicate the magnetic peaks and shoulders. All the intensities can be compared each other in the units, and the standard errors of detected neutron counts are smaller than the symbols used. The lines are guides to the eye. (d), (e) Measured inelastic neutron scattering intensity distributions in  $(h, k, l, E)$  space in an  $L$  phase (22 K) and  $O$  phase (8 K), respectively. Each set of three-abreast panels corresponds to the data for the given  $E$  measured in the  $hk0$ ,  $hk1$ , and  $hk2$  planes. The intensities were integrated over ranges of  $\pm 0.2$  rlu and  $\pm 1.0$  meV around the given  $l$  and  $E$ , respectively. The vertical tone indicates the linear scale intensity in arbitrary units in (d)–(f). The three first quadrants, boxed by white lines in the  $hk0$  planes, show areas previously reported [7]. (f) One-to-one correspondence between calculated patterns as identified by the molecular models shown in (b).

distributed over wide momentum ( $Q$ ) and energy ( $E$ ) ranges both in an  $L$  and  $O$  phase in  $\text{MgCr}_2\text{O}_4$  by inelastic neutron scattering. The overall study of spin excitations was possible because of the combination of a large single-crystal assembly, an advanced time-of-flight spectrometer with large-solid-angle detectors, and

sophisticated software to handle huge data sets in four-dimensional space.

Inelastic neutron scattering experiments were performed using the direct geometry chopper spectrometer MERLIN at the ISIS (United Kingdom) spallation neutron source [17]. The detector coverage is as large as  $-45^\circ$  to  $135^\circ$  in

the horizontal plane and  $\pm 30^\circ$  in the vertical direction. The incident energy ( $E_i$ ) was fixed at 50 meV with a chopper speed of 400 Hz. The energy resolution under elastic conditions was approximately 5% of  $E_i$ . Single-crystal rods of  $\text{MgCr}_2\text{O}_4$  were grown by a floating zone method. Details of the crystal growth are summarized in Ref. [18]. The rod was about 4 mm in diameter and 40 mm in length. Six coaligned single crystals were fixed by thin aluminum plates and inserted in a closed-cycle  $^4\text{He}$  refrigerator with  $^4\text{He}$  exchange gas. Since the spin system is three-dimensional, as shown in Fig. 1(a), the data were recorded while rotating the crystal in  $1^\circ$  steps about the vertical axis, which is unlike experiments on two-dimensional and one-dimensional systems with a fixed crystal angle ( $\omega$ ) [19,20]. The huge combined data sets were handled by the HORACE software of ISIS [21].

Figure 1(c) shows the  $E$  spectra of  $Q$ -integrated intensity, measured in an  $L$  phase (22 K) and  $O$  phase (8 K). In neutron scattering, the magnetic scattering intensity decreases by a magnetic form factor while the phonon intensity increases in proportion to  $Q^2$  with increasing  $Q$  [22]. Since below  $\sim 20$  meV, the low- $Q$  intensity is higher than the high- $Q$  intensity, as shown in Fig. 1(c), the signals in this low-energy region are magnetic in origin. As shown in the left panel, a single quasielastic mode seems to exist above  $T_N$ . In contrast, as shown in the right panel, peaks around 4.5 and 9.0 meV and tiny shoulders around 13.5 and 18.0 meV are observed below  $T_N$ , which are of an equal energy interval.

Despite the appearance of a single mode, we investigated the scattering intensity distributions in a  $Q$  space sliced at the four characteristic  $E$ 's not only below but also above  $T_N$ , as shown in Figs. 1(d) and 1(e), respectively. Above  $T_N$  [Fig. 1(d)], different patterns spreading over several reciprocal lattice units (rlu) appear at 9.0, 13.5, and 18.0 meV in addition to the zero-energy hexamer patterns at 4.5 meV, indicating the existence of other extremely short-range correlation modes. Further, as shown in Fig. 1(e), all the modes are sustained below  $T_N$ : the 4.5 meV patterns are almost identical. Each 9.0 meV pattern above  $T_N$  is regarded as a superposition of the 4.5 meV pattern and the heptamer 9.0 meV pattern below  $T_N$  and, thus, the heptamer mode certainly exists both below and above  $T_N$ , and the remaining 13.5 and 18.0 meV patterns above  $T_N$  are smeared compared with those below  $T_N$  but are essentially the same. Here, the 4.5 and 9.0 meV patterns below  $T_N$  are consistent with the previous report [7]. Thus, in the  $L$  phase with the zero-energy mode, we found multiple finite-energy short-range correlation modes, all of which are also in common with the  $O$  phase. The appearance of a single mode is due to superposition of all the modes that are broader in  $E$  compared to the  $O$  phase.

Next, to extract information on the spatial correlations of these modes, we tried to reproduce the experimental  $Q$  patterns as two-body correlation functions of classical spins, as in Refs. [7,9]. The Watson-Freeman magnetic

form factor of  $\text{Cr}^{3+}$  [23] and the orientation average over the equivalent directions were also taken into account. Through trial and error, heptamer variation models were also found for the third and fourth modes, as shown in Fig. 1(b), and the corresponding calculated patterns [Fig. 1(f)] are in agreement with those of Figs. 1(d) and 1(e). Further, the total exchange interaction energy evaluated from the numbers of antiferromagnetic (AF) and ferromagnetic (F) nearest-neighbor bonds is of equal interval as follows, which is also in agreement with experiments: the energy for each molecule can be evaluated to be  $-6J_1$ ,  $-4J_1$ ,  $-2J_1$ , and  $0J_1$  with an equal interval of  $2J_1$ , where  $J_1 > 0$  denotes an AF first-neighbor exchange interaction energy; this first-neighbor exchange interaction has been reported to be predominant over other exchange interactions in band calculations [24]. However, it is uncertain whether these are a unique solution.

The same analysis can also reproduce the previous neutron data on other spinels  $\text{HgCr}_2\text{O}_4$  and  $\text{GeCo}_2\text{O}_4$ , which are characterized as an AF  $J_1 > 0$  and AF  $J_2$  system and a F  $J_1$  and AF  $J_3$  system, respectively, [11,13]. That is, as models to explain the experimental  $Q$  patterns of zero-energy modes, the same analysis also showed that  $\text{HgCr}_2\text{O}_4$  exhibits the same hexamers consisting of first-neighbor spins (hex-I) and another hexamer consisting of second-neighbor spins (hex-II) [11] and  $\text{GeCo}_2\text{O}_4$  exhibits di-tetramers [13]. In addition, for a finite-energy mode in  $\text{GeCo}_2\text{O}_4$  assigned to tetramers [13], we have confirmed that the present analysis gives the same patterns as those obtained in the previous different analysis. Furthermore, the energetic relations agree with the evaluation from the numbers of exchange bonds as follows. The hex-I and hex-II energies are nearly degenerate experimentally [11], which are evaluated to be  $-6J_1 + 6J_2$  and  $-6J_2$ , respectively; thus, the degeneracy is ascribed to the plausible assumption of  $J_1 \approx 2J_2$ . The tetramer energy is higher than the di-tetramer one experimentally [13], which are evaluated to be  $-2J_1$  and  $11J_1 - 4J_3$ , respectively; thus, the relation means  $J_3 > 3.25J_1$  that is satisfied in sign.

To summarize the aforementioned results, the present experiments found a common hierarchical set of spin excitations ranging from the zero-energy mode to the finite-energy modes above and below  $T_N$ , which can be described by the hexamer and heptamer variation models. Now we turn to the significance of this finding. First, existence both above and below  $T_N$  means that the molecular spin excitations are neither caused by static magnetic long-range ordering nor likely to be normal spin waves arising from the magnetic order. In addition, the spin-lattice order is tetragonal [14,15], whereas the hexamers and heptamers are trigonal, as shown in Fig. 1(a); they are also different in symmetry. This difference in symmetry has been very recently detected by ultrasound measurements in the  $L$  phase: there are tetragonal spin excitations or fluctuations below  $\sim 3.4$  meV originating from spin Jahn-Teller

coupling with the tetragonal spin-lattice order and two types of trigonal spin excitations around  $\sim 3.4$  meV and in the higher-energy region, corresponding to the hexamer and the heptamer variations, respectively [25].

Second, we focus on the finding that the finite-energy modes are spatially confined, as is the zero-energy mode. The spatially confined zero-energy mode is recognized as being the direct result of high degeneracy in the ground states, which restricts the formation of a normal wavelike magnetic order that is inevitably longer than the wavelength of the propagation vector. In analogy to this, the spatially confined finite-energy modes suggest high degeneracy in excited states, or the expanded concept of frustration in excitations. Indeed, this concept seems to be realized in the  $O$  phase, which exhibits a complex magnetic structure with multiple propagation vectors and 32 magnetic ions in its unit cell [14,15], implying that 32 spin wave modes are squeezed in an energy region. This situation is most probably a clearer example of the term “frustration effect in excitations” mentioned in the previous report [7]. Similarly, in the  $L$  phase without a magnetic order, since the concept of a unit cell is broken down or a unit cell with the larger numbers of magnetic ions can be defined, further higher degeneracy is expected in the spin excited states. Thus, one can conclude that although the molecular modes might have originally been normal spin waves, the expanded frustration transforms them beyond recognition.

Third, we discuss why the  $L$  phase sustains the molecular spin excitations as well as in the  $O$  phase. This commonality requires that the  $L$  phase ground state (zero-energy mode providing the basis of the excitations) is spatially larger than the finite-energy excitations. However, the  $L$  phase zero-energy hexamers are rather smaller than the finite-energy heptamers. On the other hand, interestingly, the aforementioned ultrasound data suggest that the true zero-energy mode is mainly described by not trigonal hexamers but other tetragonal dynamical short-range correlations or their crossover [25]. The tetragonal correlations are probably a precursor of the  $O$  phase spin order, which generates many magnetic Bragg points represented by multiple propagation vectors  $(1, 0, 1/2)$ ,  $(1/2, 1/2, 0)$ , and  $(1, 0, 0)$  on and near the Brillouin zone boundary [14,15], though obviously the whole boundary cannot be encompassed by only the finite points. Thus, the observed  $Q$  patterns of the zero-energy mode could be reinterpreted as the crossover of the hexamers and an assembly of rather small spots with the vectors, and  $Q$  widths (correlation lengths) of the spots are smaller (larger) than those of the molecules. We also remark that such a many- $Q$  assembly picture was used in works for  $\text{ZnCr}_2\text{O}_4$  [8] and another frustrated  $\text{NiS}_2$  [26].

Last, we discuss the ramifications of this expanded concept. The concept is realized when a unit cell consists of many components. However, in contrast, from a mean-field theory for pyrochlore systems with only four magnetic

sublattices, it was reported that only ground states are highly degenerate and that this is not the case for excited states [27]. This, in turn, suggests that the expanded concept can also be applied to atomic liquids and amorphous systems, which are similar to spin frustrated systems as follows: a spin-frustrated system exhibits, for example, a spin glass state because of the presence of trace impurities [28], which is comparable to a supercooled liquid that undergoes a glass transition upon experiencing a small impact. Further, supercooled liquids and glasses exhibit similar resonancelike short-range vibrational modes called boson peaks. Interestingly, a recent x-ray spectroscopic study revealed that boson peaks are originally identical to, but are then severely transformed from, lattice waves propagating in a crystal (phonons), and also suggested that the  $Q$  correlations are distributed over several rlu near the pseudo-Brillouin zone boundary [29].

In summary, we studied spin excitations over a wide  $(Q, E)$  space in the frustrated spinel magnet  $\text{MgCr}_2\text{O}_4$  by single-crystal time-of-flight inelastic neutron scattering. A set of molecular spin excitation modes was commonly observed above and below  $T_N$ . This observation leads us to the concept of frustration in excitations, which is applicable both above and below  $T_N$  and in other spinel magnets  $\text{HgCr}_2\text{O}_4$  and  $\text{GeCo}_2\text{O}_4$ , and probably also in atomic liquids, complex ordered systems, and amorphous systems. Our work will promote the comparative studies of local spin or lattice modes, normal spin waves, phonons, and their novel couplings in complex systems, which could not be presently detected. The complementary use of a triple axis spectrometer would provide the detailed information in the future.

We thank Professors T. Masuda and T.J. Sato for the fruitful discussions and Mr. M. Onodera for providing assistance at Tohoku University. This study was financially supported by Grants-in-Aid for Young Scientists (B) (22740209), Priority Areas (22014001), and Scientific Researches (S) (21224008) from the MEXT of Japan.

---

\*tomiyasu@m.tohoku.ac.jp

- [1] L. D. Landau and E. M. Lifshitz, *Course of Theoretical Physics Statistical Physics Part 2* Vol. 9 (Pergamon, Oxford, 1981).
- [2] R. P. Feynman, *Phys. Rev.* **94**, 262 (1954).
- [3] M. J. P. Gingras, *Science* **326**, 375 (2009).
- [4] G. H. Wannier, *Phys. Rev.* **79**, 357 (1950).
- [5] P. W. Anderson, *Phys. Rev.* **102**, 1008 (1956).
- [6] H. Ueda, H. Mitamura, T. Goto, and Y. Ueda, *Prog. Theor. Phys. Suppl.* **159**, 256 (2005).
- [7] K. Tomiyasu, H. Suzuki, M. Toki, S. Itoh, M. Matsuura, N. Aso, and K. Yamada, *Phys. Rev. Lett.* **101**, 177401 (2008).
- [8] P. H. Conlon and J. T. Chalker, *Phys. Rev. B* **81**, 224413 (2010).
- [9] S.-H. Lee, C. Broholm, W. Ratcliff, G. Gasparovic, Q. Huang, T. H. Kim, and S.-W. Cheong, *Nature (London)* **418**, 856 (2002).

- [10] J.-H. Chung, M. Matsuda, S.-H. Lee, K. Kakurai, H. Ueda, T.J. Sato, H. Takagi, K.-P. Hong, and S. Park, *Phys. Rev. Lett.* **95**, 247204 (2005).
- [11] K. Tomiyasu, H. Ueda, M. Matsuda, M. Yokoyama, K. Iwasa, and K. Yamada, *Phys. Rev. B* **84**, 035115 (2011).
- [12] Y. Yasui, M. Kanada, M. Ito, H. Harashina, M. Sato, H. Okumura, K. Kakurai, and H. Kadowaki, *J. Phys. Soc. Jpn.* **71**, 599 (2002).
- [13] K. Tomiyasu, M. K. Crawford, D. T. Adroja, P. Manuel, A. Tominaga, S. Hara, H. Sato, T. Watanabe, S. I. Ikeda, J. W. Lynn *et al.*, *Phys. Rev. B* **84**, 054405 (2011).
- [14] H. Shaked, J. M. Hastings, and L. M. Corliss, *Phys. Rev. B* **1**, 3116 (1970).
- [15] S. Ji, S.-H. Lee, C. Broholm, T. Y. Koo, W. Ratcliff, S.-W. Cheong, and P. Zschack, *Phys. Rev. Lett.* **103**, 037201 (2009).
- [16] Y. Horibe, M. Shingu, K. Kurushima, H. Ishibashi, N. Ikeda, K. Kato, Y. Motome, N. Furukawa, S. Mori, and T. Katsufuji, *Phys. Rev. Lett.* **96**, 086406 (2006).
- [17] R. Bewley, R. Eccleston, K. McEwen, S. Hayden, M. Dove, S. Bennington, J. Treadgold, and R. Coleman, *Physica (Amsterdam)* **B385-386**, 1029 (2006).
- [18] Y. Kousaka, K. Tomiyasu, T. Yokobori, K. Horigane, H. Hiraka, K. Yamada, and J. Akimitsu, *J. Phys. Conf. Ser.* **320**, 012040 (2011).
- [19] J. M. Tranquada, H. Woo, T. G. Perring, H. Goka, G. D. Gu, G. Xu, M. Fujita, and K. Yamada, *Nature (London)* **429**, 534 (2004).
- [20] M. Arai, M. Fujita, M. Motokawa, J. Akimitsu, and S. M. Bennington, *Phys. Rev. Lett.* **77**, 3649 (1996).
- [21] T. G. Perring, R. A. Ewings, and J. V. Duijn, HORACE: Visualising and Manipulating  $S(\mathbf{Q}, \omega)$  Measured in all Four Dimensions, <http://horace.isis.rl.ac.uk>.
- [22] W. Marshall and S. W. Lovesey, *Theory of Thermal Neutron Scattering* (Oxford University Press, Oxford, 1971).
- [23] R. E. Watson and A. J. Freeman, *Acta Crystallogr.* **14**, 27 (1961).
- [24] A. N. Yaresko, *Phys. Rev. B* **77**, 115106 (2008).
- [25] T. Watanabe, S.-I. Ishikawa, H. Suzuki, Y. Kousaka, and K. Tomiyasu, *Phys. Rev. B* **86**, 144413 (2012).
- [26] M. Matsuura, Y. Endoh, H. Hiraka, K. Yamada, A. S. Mishchenko, N. Nagaosa, and I. V. Solovyev, *Phys. Rev. B* **68**, 094409 (2003).
- [27] J. N. Reimers, A. J. Berlinsky, and A.-C. Shi, *Phys. Rev. B* **43**, 865 (1991).
- [28] W. Ratcliff, S.-H. Lee, C. Broholm, S. W. Cheong, and Q. Huang, *Phys. Rev. B* **65**, 220406(R) (2002).
- [29] A. I. Chumakov, G. Monaco, A. Monaco, W. A. Crichton, A. Bosak, R. Ruffer, A. Meyer, F. Kargl, L. Comez, D. Fioretto *et al.*, *Phys. Rev. Lett.* **106**, 225501 (2011).